Journal of Medicinal Chemistry

Article

pubs.acs.org/jmc

Identification of a Class of Novel Tubulin Inhibitors

Xin Yi,[†] Bo Zhong,[†] Kerri M. Smith,[†] Werner J. Geldenhuys,[§] Ye Feng,[†] John J. Pink,[∥] Afshin Dowlati,[⊥] Yan Xu,[†] Aimin Zhou,[†,‡] and Bin Su*[,†,‡]

[†]Department of Chemistry and [‡]Center for Gene Regulation in Health and Disease, College of Sciences and Health Professions, Cleveland State University, 2121 Euclid Avenue, Cleveland, Ohio 44115, United States

[§]Department of Pharmaceutical Sciences, Northeast Ohio Medical University, 4209 State Route 44, Rootstown, Ohio 44272, United States

[∥]Division of General Medical Sciences—Oncology and [⊥]Division of Hematology and Oncology, Case Western Reserve University School of Medicine, 10900 Euclid Avenue, Cleveland, Ohio 44106, United States

ABSTRACT: We previously developed a series of anticancer agents based on cyclooxygenase-2 (COX-2) inhibitor nimesulide as a lead compound. However, the molecular targets of these agents still remain unclear. In this study, we synthesized a biotinylated probe based on a representative molecule of the compound library and performed protein pull-down assays to purify the anticancer targets of the compound. Via proteomic approaches, the major proteins bound to the probe were identified to be tubulin and heat shock protein 27 (Hsp27), and the compound inhibited tubulin polymerization by binding at the colchicine domain. However, the tubulin inhibitory effect of the compound activated the Hsp27 phosphorylation and possibly overrode the direct Hsp27 inhibitory effects, which made it difficult to solely validate the Hsp27 target. Taken together, the compound was a dual ligand of tubulin and Hsp27, inhibited tubulin polymerization, and had the potential to be a class of new chemotherapeutic agents.

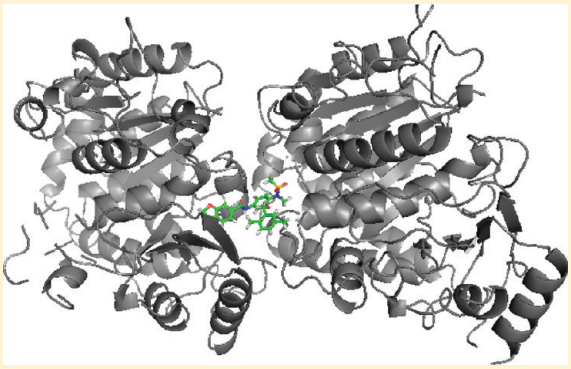

1. INTRODUCTION

Tubulin-containing structures are important for many important cellular functions, including chromosome segregation during cell division, intracellular transport, development, and maintenance of cell shape, cell motility, and distribution of molecules on cell membranes.[1] The rapid growth of cancer cells leads to their high dependence on tubulin polymerization/depolymerization, which makes tubulin a good target for anticancer drug development. Paclitaxel (Taxol), the representative tubulin inhibitor approved by the Food and Drug Administration (FDA) in 1992 for cancer treatment, is one of the most powerful chemotherapeutic agents currently in use. Paclitaxel binds to tubulin and results in its precipitation and sequestration, which interrupt many important biological functions of cancer cells that depend on a dynamic tubulin polymerization and depolymerization process.[2] This explains the high potency and efficacy of paclitaxel in fighting cancer.

Besides paclitaxel, FDA also approved other tubulin inhibitors with complex structures for cancer treatment including epothilone analogues, vinca alkaloid analogues, and halichondrin analogues (Figure 1). Treatment with tubulin inhibitors has led to improvement in the duration and quality of life for many cancer patients.[3] However, most of them eventually develop progressive disease after initially responding to the treatment.[4−6] Drug resistance of most tubulin inhibitors represents a major obstacle to overcome in order to improve the long-term response and survival of cancer patients.[4] In addition to the resistance issue, neurotoxicity is one of the major side effects of the tubulin inhibitors derived from complex natural products, which affects the quality of life of cancer patients.[7−9] Furthermore, low oral-bioavailability limits the convenient oral drug administration.[10] There is an urgent need to develop new tubulin inhibitors with fewer side effects and with good oral bioavailability and that are less prone to the development of resistance.

There are three well-documented binding domains of tubulin, which can be utilized to design new tubulin inhibitors. The first binding domain is the pocket for taxanes and epothilones.[11,12] The second domain is the pocket for vinca alkaloids and halichondrins.[13,14] FDA approved tubulin inhibitors binding to these two domains all are derivatives of complex natural products (Figure 1). These compounds have very diverse structures but share the same characteristics: high bulkiness, hydrophobicity, and complicated structure. In addition, they tend to be easily recognized by P-glycoprotein and pumped out of cancer cells, which cause drug resistance.[3−5,15] The potential to develop better tubulin inhibitors binding at these two domains therefore appears to be limited.

The third binding domain of tubulin is the pocket for colchicine, a small natural product with a relatively simple

Received: January 23, 2012
Published: March 21, 2012

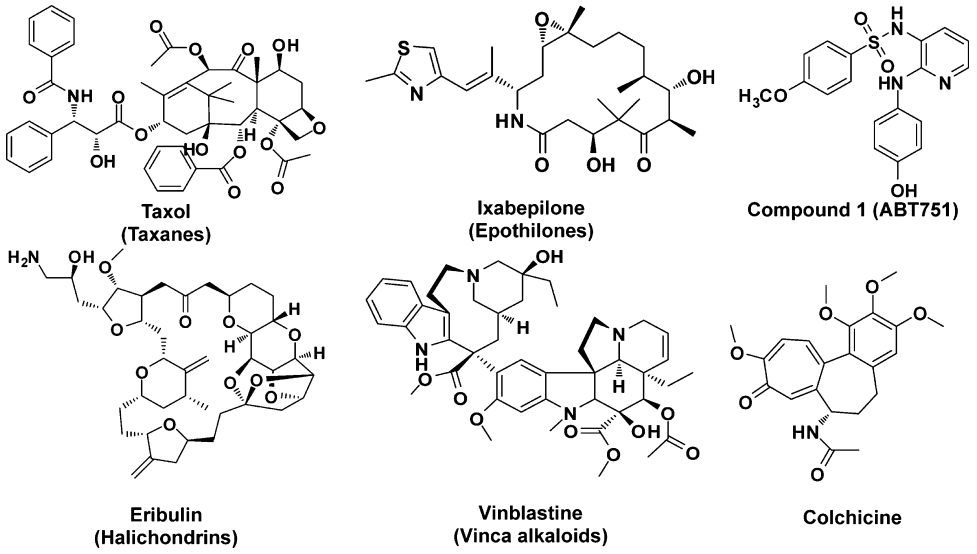

Figure 1. Structures of the classic tubulin inhibitors.

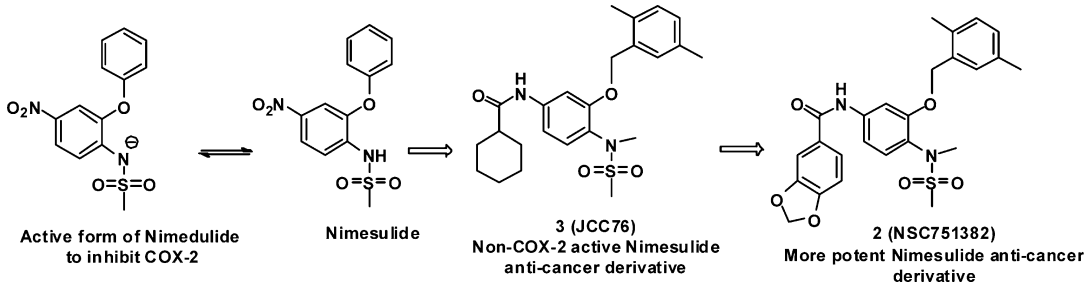

Figure 2. From COX-2 inhibitor nimesulide to potent anticancer agent **2**.

structure (Figure 1). So far, there are no FDA approved anticancer drugs targeting this domain.[3] Colchicine is clinically used as a monotherapy for the treatment of familial Mediterranean fever and acute gout flares but not as a cancer therapy because of its high toxicity. Efforts have been made to develop less toxic candidates targeting the colchicine binding domain. Some synthetic small molecules targeting this domain such as compound **1**, *N*-[2-[(4-hydroxyphenyl)amino]-3-pyridinyl]-4-methoxybenzenesulfonamide (ABT-751)[3] (Figure 1), are in clinical trials as cancer treatment.[3,16−18] Their unique capability to inhibit the growth of multiple drug resistant (MDR) tumor cell lines, lower neurotoxicity, and good oral bioavailability are their primary advantages, compared to the currently FDA approved tubulin inhibitors.[16−18] Drug development of compound **1** demonstrated the potential of colchicine domain binders as better tubulin inhibitors.[16−18]

To develop new tubulin inhibitors, it traditionally starts with a lead compound binding to a certain domain of tubulin but with relatively weak activity. Structural optimization will be performed to increase the binding affinity and the anticancer activity of the lead compound. In the current study, we describe the development of a novel tubulin inhibitor via a different approach to the traditional drug development. We synthesized a class of anticancer agents without knowing their molecular targets. However, the antiproliferation activity guided drug optimization dramatically improved the cell growth inhibitory activity of the lead compound, a COX-2 inhibitor nimesulide.[19,20] A very potent compound **2**, benzo[1,3]dioxole-5-carboxylic acid [3-(2,5-dimethylbenzyloxy)-4-(methanesulfonylmethylamino)-phenyl]amide (NSC751382)[20] developed in our previous study, showed very promising anticancer activity and suppressed the growth of various cancer cell lines with IC_{50}s of 0.1−0.5 μM.[20] In the current study, we identified the molecular targets of compound **2** as tubulin and heat shock protein 27 (Hsp27) via proteomic and chemical biology approaches. The compound was proved to be a colchicine domain binder and exhibited potent tubulin polymerization inhibitory activity. The direct biological response of Hsp27 after the compound treatment was difficult to determine because of the unclear downstream cellular signals and also the indirect effects of tubulin inhibition on Hsp27. Nevertheless, there is a great potential to develop a class of novel tubulin inhibitors based on our discovery. Our drug discovery process also demonstrates that ligand based lead optimization via traditional medicinal chemistry is an effective strategy to improve the cell proliferation inhibitory activity of the lead compound. More potent derivatives make the target identification easier, since they should have a much higher binding affinity with their target(s). Further optimization based on the identified targets could involve computational chemistry if the binding domain is well-defined and could greatly speed up the drug development.

2. RESULTS AND DISCUSSION

2.1. Origin of Compound 2 and the Construction of Its Biotinylated Probe. Compound **2** is a potent anticancer agent structurally derived from the COX-2 inhibitor nimesulide (*N*-(2-phenoxy-4-nitrophenyl)methanesulfonamide).[20] Numerous studies have demonstrated the anticancer activity of nimesulide.

dx.doi.org/10.1021/jm300100d | J. Med. Chem. 2012, 55, 3425−3435

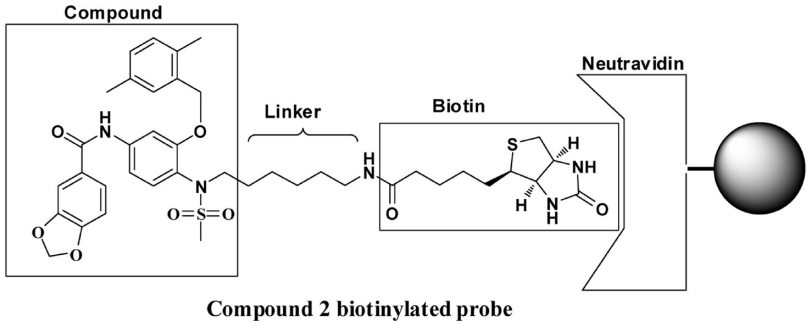

Figure 3. Structure of compound **2** probe.

Scheme 1[a]

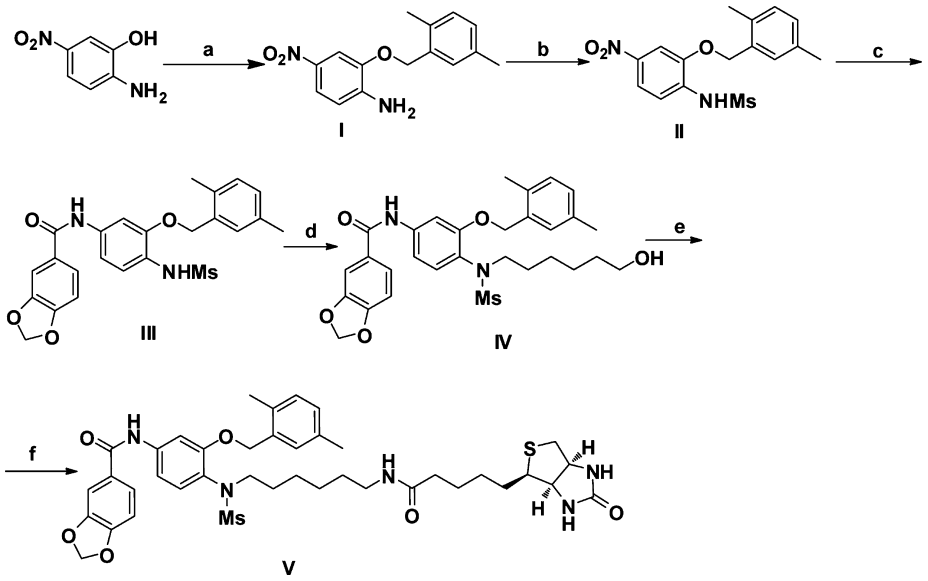

[a]Regents and conditions: (a) 2,5-dimethylbenzyl bromide, K_2CO_3, DMF; (b) (1) MsCl, NaH, DMF; (2) NaOH, MeOH; (c) (1) $FeCl_3$, Zn, DMF/H_2O; (2) piperonyloyl chloride, K_2CO_3, 1,4-dioxane; (d) 6-bromo-1-hexanol, K_2CO_3, DMF; (e) (1) MsCl, Et_3N, DCM; (2) $NH_3 \cdot H_2O$, EtOH; (f) (+)-D-biotin, PyBOP, Et_3N, DMF.

However, the nimesulide concentrations used in these studies ranged from 200 to 500 μM, which greatly exceeded the concentration necessary to inhibit COX-2 activity.[21−26] This line of reasoning suggests that nimesulide targeted other pathways in order to achieve anticancer activity, and blockage of these pathways required much higher concentrations. This supported the hypothesis that nimesulide inhibited cancer cell growth and induced apoptosis independent of its effects on COX-2.[22,23,27] Structurally, the ionization of the sulfonamide group of nimesulide was critical for its COX-2 inhibition (Figure 2).[28,29] The N-methylation of nimesulide blocked the ionization of the sulfonamide group, which abolished the COX-2 inhibitory activity.[28,29] Nimesulide showed minor hepatotoxicity after long-term usage because of the multistep nitroreductive bioactivation that produced the hazardous nitro anion radical and nitroso intermediate of the nitro group.[30] The conversion of the nitro group could erase the potential hepatotoxicity of the new analogues. These two critical modifications eliminated the COX-2 inhibitory activity and the hepatotoxicity, but it was not clear if the anticancer activity would be improved. After extensive investigations, we obtained our first generation non-COX-2 active nimesulide anticancer derivative **3**, *N*-(3-(2,5-dimethylbenzyloxy)-4-(methylmethylsulfonamido)phenyl)cyclohexanecarboxamide (JCC76) (Figure 2).[19,31,32] It inhibited SKBR-3 breast cancer cell growth with an IC_{50} of 1.38 μM, which was about 100-fold more active than nimesulide. Furthermore, compound **2** was recently developed based on compound **3** and has demonstrated greater anticancer potency,[20] with IC_{50} of 0.1−0.5 μM to inhibit cancer cell growth. However, the specific molecular targets of compounds **3** and **2** were still unclear.

Target identification represents a major challenge in anticancer drug development. The generally used method is to immobilize the compound via a chemical linker on a solid-phase support, followed by affinity purification of the cellular targets (Figure 3).[33] Therefore, we designed and synthesized biotin-linked compound **2** as a probe for the target identification (Scheme 1).[34] Biotinylated compound **2** showed acceptable antiproliferative activity on SKBR-3 breast cancer cells (IC_{50} = 2 μM), although the anticancer activity is lower than that of the parental compound with an IC_{50} of 0.2 μM.[20]

2.2. Affinity Purification of Compound 2-Bound Proteins. We hypothesized that compound **2** bound to certain proteins to achieve its anticancer activity. We mixed compound **2** probe with SKBR-3 breast cancer cell lysate in order to allow specific binding proteins to attach to the compound **2** moiety of the probe. For the protein isolation, the biotin moiety of the probe was bound to the neutravidin resin to immobilize the

dx.doi.org/10.1021/jm300100d | J. Med. Chem. 2012, 55, 3425−3435

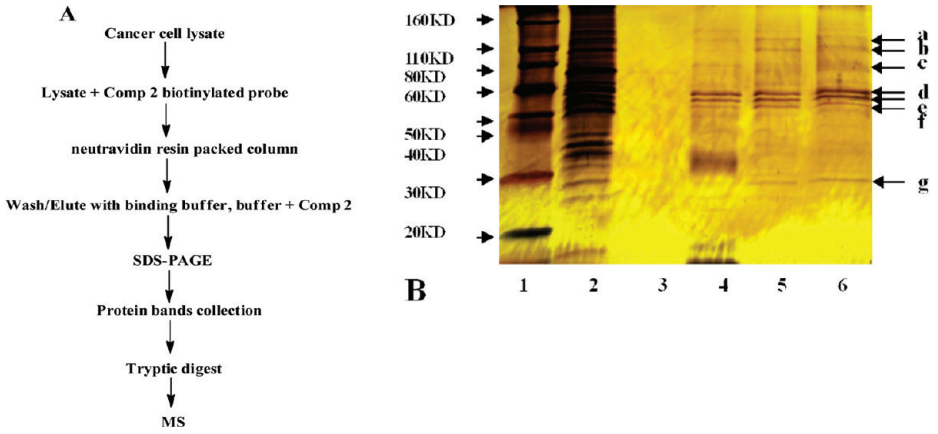

Figure 4. Affinity isolation of **2**-binding proteins. (A) Procedure for the purification of compound **2** binding proteins. (B) SKBR-3 breast cancer cell lysate exposed to the probe (final probe concentration in the lysate was 25 μM) was incubated for 1 h at room temperature and then incubated with neutravidin resin for 30 min. The mixture was loaded on a separation column and centrifuged. The resin was washed with binding buffer 5 times. The last wash elution solution was kept. The resin was further washed twice with buffer containing different concentrations of compound **2**. The last buffer without drug wash solution (lane 3), two times wash solution with compound **2** (lane 5 and 6), and the resin (lane 4) were denatured in SDS sample buffer and separated by SDS–PAGE. Lane 1 represents the molecular weight markers, and lane 2 is the whole cell lysate. Visualization of the separated proteins with silver stain showed the specific binding proteins with compound **2**.

probe. After extensive washing with binding buffer, the nonbinding proteins were eluted. Then compound **2** was used as a competing agent to wash the immobilized probe, and the proteins specifically binding to the probe at the compound **2** domain were pulled out. The main procedure is described in Figure 4A. We next examined the molecule weight of the binding proteins using sodium dodecyl sulfate–polyacrylamide gel electrophoresis (SDS–PAGE) and stained the gel with silver staining reagent (Figure 4B). Lane 2 is the cell lysate, and lane 3 is the final elution solution. Lane 5 is the binding buffer with compound **2** (25 μM) as elution solution. Lane 6 is binding buffer with compound **2** (50 μM) as elution solution, and lane 4 is the resin boiled with SDS buffer. The results suggest that compound **2** was not competitive enough to pull all the proteins out of the probe, and the resin with the probe still held a good amount of proteins. It is also possible that the competition experiment was finished on the resin packed column and only lasted 30 min, which led to less effective competition. There are seven visible protein bands that can be identified on the gel. Protein **a** and **b** have molecular weights above 110 kDa, protein **c** has a molecular weight about 80 kDa, proteins **d**, **e**, and **f** have molecular weights about 55–60 kDa, and protein **g** has a molecular weight about 28 kDa. Apparently, **d** and **e** are the major proteins bound to compound **2**; the other proteins are relatively minor. However, it is too early to speculate which protein(s) is (are) the role player(s) at this stage. Minor attached proteins are not less important than the highly binding proteins. We will identify all the visible proteins on the gel in next step.

2.3. Identification of the Binding Proteins. Compound **2** binding proteins were separated by SDS–PAGE and collected by cutting the gel with the visible protein bands. After silver-staining agent was removed, the protein bands were subjected to tryptic digestion in situ. The resulting peptide mixture was identified with mass spectrometry. The molecular weight of the peptide mass fingerprint was used to identify the protein identity via Mascot database (Matrix Science Mascot, Boston, MA). The proteins with the best score (highest possibility) are listed in Table 1. Band a was identified to be the trypsin residue, which is possibly the signal of the leftover trypsin in the digestion step, and band a itself did not give any countable signals. Bands b, c, and f were keratin proteins with peptide mass fingerprint matching scores below 10%. These low binding, and without clear functions related to cell growth proteins are not listed in Table 1. The major bands d and e were identified to be tubulin α and tubulin β, respectively. Band g was identified to be Hsp27. Both proteins are very critical for cancer cell proliferation.[35] To confirm the protein identity, we repeated the SDS–PAGE assay combined with Western blot (Figure 5A). The binding proteins were confirmed by using the corresponding antibodies. Tubulin and Hsp27 as molecular targets are new observations for the non-COX-2 active nimesulide anticancer derivatives. It was reported that tubulin has relatively strong interaction with Hsp27, and the two proteins could be co-precipitated in the immunoprecipitation experiment.[36] In our study, both proteins were pulled out by the probe, which could be due to the interaction between the two proteins. The probe might only bind either to tubulin or to Hsp27, but the interaction between the two proteins could have caused them to both be retained by the probe. To rule out the possibility of co-precipitation, we used tubulin and Hsp27 pure proteins and our probe to repeat the binding experiments individually. The protein binding ability was determined with Western analysis (Figure 5B). After 5 times extensive washing with binding buffer, the extra proteins were all eluted and there were no proteins detected in the fifth elution solution. However, tubulin and Hsp27 were further eluted after **2** was added in the elution solution. The results indicated that both proteins could specifically bind to the probe and could be eluted with buffer containing compound **2**, suggesting that compound **2** was the ligand for both proteins. Tubulin inhibitor **1** with a sulfonamide moiety is a colchicine domain binder.[18] Because of the structure similarity between compound **2** and **1** (Figure 1), we speculated that compound **2** might also be a colchicine domain binder. To prove our hypothesis, we preincubated tubulin protein with an equivalent amount of colchicine for 1 h and then repeated the experiment. We found that the probe did not hold any tubulin protein (Figure 5B), suggesting that compound **2** and colchicine share same binding site and that colchicine has higher binding affinity in the

dx.doi.org/10.1021/jm300100d | J. Med. Chem. 2012, 55, 3425–3435

Table 1. Peptides Were Sequenced by Electrospray Ionization Quadrupole Time-of-Flight Tandem Mass Spectrometry, and Internal Sequences Were Searched Using the Mascot Database

protein band	molecular weight (estimated based on the marker), kDa	peptides (bold and underlined) matching with potential protein	% of the matching	protein identity
d	58	MRECISIHVG QAGVQIGNAC WELYCLEHGI QPDGQMPSDK **TIGGGDDSFN TFFSETGAGK** HVPR**AVFVDL EPTVIDEVR**T GTYRQLFHPE QLITGKEDAA NYARGHYTI GK**EIIDLVLD R**IRKLADQCT GLQGFLVFHS FGGGTGSGFT SLLMERLSVD YGKKSKLEFS IYPAPQVSTA VVEPYNSILT THTTLEHSDC AFMVDNEAIY DICRRNLDIE RPTYTNLNR**L ISQIVSSITA** **SIR**FDGALNV DLTEFQTNLV PYPRIHFPLA TYAPVISAEK AYHEQLSVAE ITNACFEPAN QMVKCDPRHG KYMACCLIYR GDVVPKDVNA AIATIKTKRS IQFVDWCPTG FK**VGINYQPP TVVPGGDLAK** VQRAVCMLSN TTAIAEAWAR LDHKFDLMYA KR**AFVHWYVG EGMEEGEFSE AR**EDMAALEK DYEEVGVDSV EGEGEEEGEE Y	21	bovin tubulin α chain
e	55	MREIVHIQAG QCGNQIGAKF WEVISDEHGI DPTGTYHGDS DLQLDR**ISVY YNEATGGK**YV PR**AILVDLEP GTMDSVR**SGP FGQIFRPDNF VFGQSGAGNN WAK**GHYTEGA ELVDSVLDVV R**KEAESCDCL QGFQLTHSLG GGTGSGMGTL LISKIREEYP DRIMNTFSVV PSPKVSDTVV EPYNATLSVH QLVENTDETY CIDNEALYDI CFRTLKLTTP TYGDLNHLVS AIMSGVTTCL RFPGQLNADL R**KLAVNMVPF PR**LHFFMPGF APLTSRGSQQ YR**ALTVPELT QQVFDAK**NMM AACDPRHGRY **LTVAAVFR**GR MSMKEVDEQM LNVQNK**NSSY FVEWIPNNVK** TAVCDIPPRG LKMAVTFIGN STAIQELFKR **ISEQFTAMFR** RKAFLHWYTG EGMDEMEFTE AESNMNDLVS EYQQYQDATA EEEEDFGEEA EEEA	23	bovin tubulin β chain
g	28	MTERRVPFSL LRGPSWDPFR DWYPHSR**LFD QAFGLPR**LPE EWSQWLGGSS WPGVVRPLPP AAIESPAVAA PAYSRALSR**Q** **LSSGVSEIRH** TADRWR**VSLD VNHFAPDELT VK**TKDGVVEI TGKHEERQDE HGYISRCFTR KYTLPPGVDP TQVSSSLSPE GTLTVEAPMP K**LATQSNEIT IPVTFESR**AQ LGGPEAAKSD ETAAK	25	human heat shock protein 27

Figure 5. Protein identity and binding specificity confirmed with antibodies and pure tubulin and Hsp27. (A) Protein identity was further confirmed via Western blot with tubulin and Hsp27 antibodies. SDS–PAGE assay in Figure 4 was repeated, and the protein was transferred to a PVDF membrane and probed with tubulin and Hsp27 antibodies. (B) Binding of biotinylated compound **2** with pure Hsp27, tubulin, colchicine preincubated tubulin, and paclitaxel preincubated tubulin. The proteins (separated experiments) were exposed to the probe (final probe concentration in the protein solution was 2 μM) and incubated for 1 h at room temperature and then incubated with neutravidin resin for 30 min. The mixture was loaded on a separation column and centrifuged. The resin was washed with binding buffer 5 times and then further washed twice with buffer containing different concentrations of compound **2** (25, 50 μM). All the elution solutions and the resin were denatured with SDS buffer and then separated by SDS–PAGE, transferred to a PVDF membrane, and probed with tubulin and Hsp27 antibodies.

domain than compound **2**. However, preincubation tubulin with paclitaxel did not affect the binding ability of the probe with the tubulin. These data are consistent with our hypothesis that compound **2** binds to the colchicine binding domain on tubulin. Preincubating tubulin with colchicine saturated the binding domain and blocked the probe to attach to the protein, but paclitaxel with different binding domain did not affect the binding.

2.4. Biological Activity of Compound 2 to Tubulin and Hsp27. We showed here that compound **2** binds to tubulin; however, it is still not clear if the compound can interfere with tubulin function. Tubulin can be affected in two manners. Taxanes and epothilones stabilize tubulin polymerization, whereas vinca alkaloids, halichondrins, and colchicine inhibit tubulin polymerization.[12,13,37,38] Although binding differently, colchicine and vinca alkaloids show the same mechanism of inhibition of tubulin. Compound **2**, a relatively smaller and nonchiral molecule compared to the bulky and bearing multiple chiral centers natural product tubulin interfering agents, inhibited tubulin polymerization dose-dependently (Figure 6A). Nocodazole, a well-known tubulin inhibitor, was used as a positive control for the assay. Compound **3**, the first generation nimesulide anticancer derivative, showed moderate tubulin polymerization inhibitory activity. In addition, the tubulin polymerization inhibitory effect was observed in cancer cells (Figure 6B). After 12 h of treatment with compound **2** at 0.5 and 1 μM, the microtubules were disorganized and their density was significantly

dx.doi.org/10.1021/jm300100d | J. Med. Chem. 2012, 55, 3425–3435

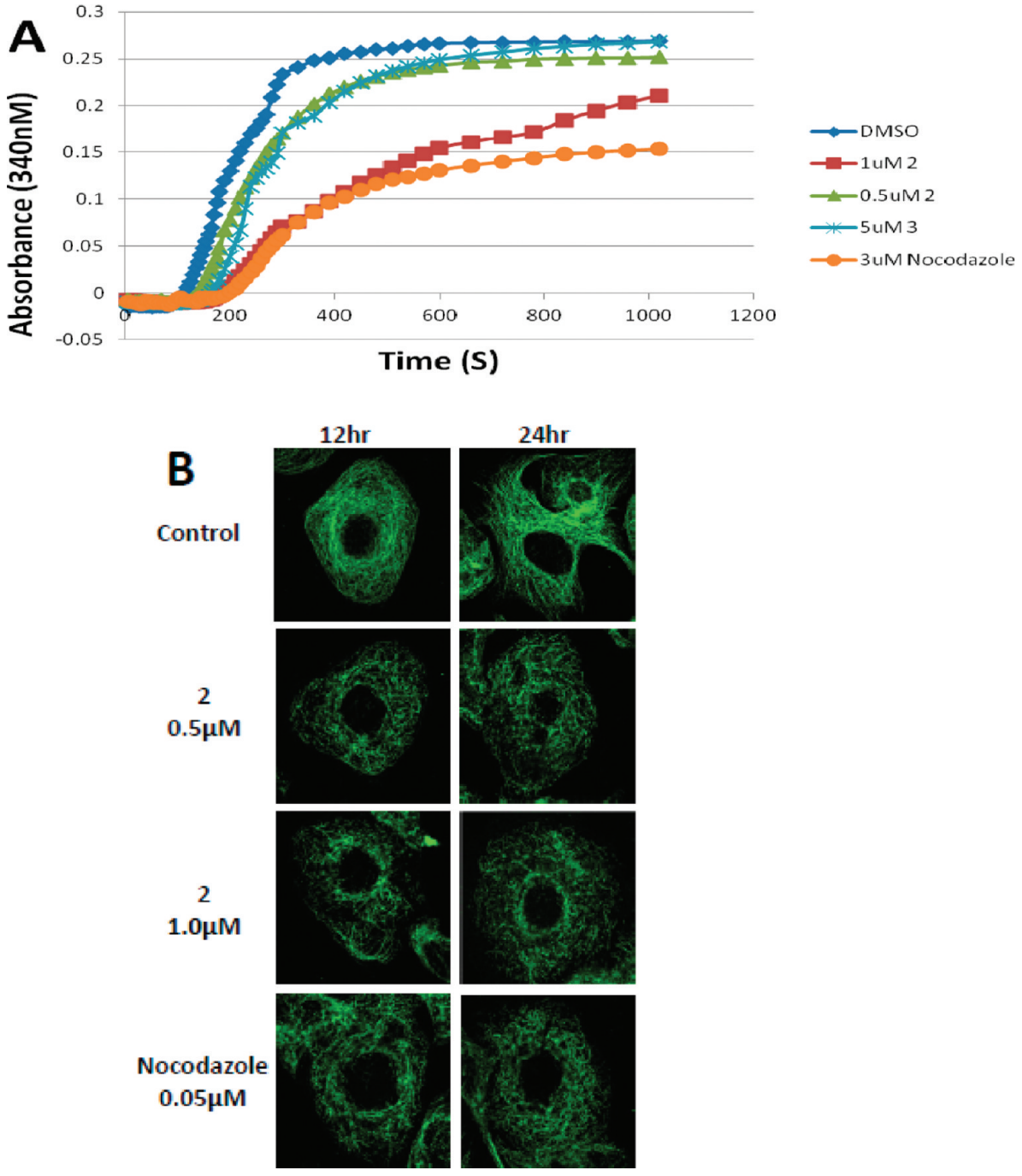

Figure 6. Effect of compound **2** on the organization of the microtubule cytoskeleton in vivo and in vitro. (A) The tubulin polymerization was done using bovine brain tubulin with an in vitro assay. MAP-rich tubulin was incubated at 37 °C in the presence of vehicle (DMSO), 3 μM nocodazole, 0.5 and 1 μM **2**, and 5 μM **3**. Absorbance at 340 nm was measured for 20 min and presented as the increased polymerized microtubule. The data were from one of two independent experiments with similar results. (B) SKBR-3 cells were incubated with 0.1% DMSO, 0.05 μM nocodazole, and 0.5 and 1 μM **2** for 12 h and 24 h. Cells were fixed, labeled with Alexa Fluor 488 antitubulin antibody, and observed with a Leica TCS SP2 fluorescence microscope.

reduced in SKBR-3 breast cancer cells. After 24 h of treatment, the effect was more pronounced. The results indicate that compound **2** could inhibit tubulin polymerization in an assay with purified protein and in SKBR-3 cells. The results also are in agreement with the cell cycle arrest studies of compound **2** in previous studies.[20]

Hsp27 is a chaperone of the small heat shock protein (sHsp) family. The common functions of small heat shock proteins are chaperone activity, thermotolerance, inhibition of apoptosis, regulation of cell development, and cell differentiation. They are also partially involved in cell signal transduction.[35,39−42] Compound **2** showed significant anticancer activity in our previous studies.[20] Tubulin inhibitory activity was responsible for the cancer cell toxic effect of the compound. Did Hsp27 play any role during the cell death since compound **2** bound to this protein? The phosphorylation of Hsp27 is the key step for Hsp27 to participate in the cell signal transduction process.[36,40] We checked the levels of phosphorylated Hsp27 and total

dx.doi.org/10.1021/jm300100d | J. Med. Chem. 2012, 55, 3425−3435

Hsp27 in SKBR-3 breast cancer cells after compound **2** treatment (Figure 7). The compound significantly increased

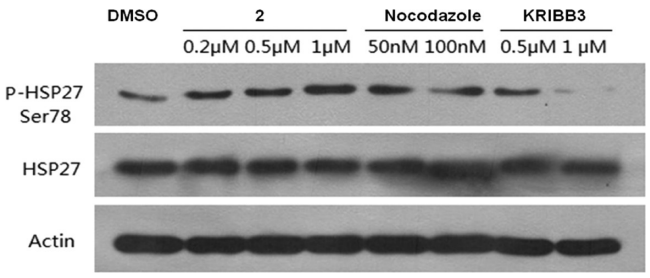

Figure 7. Effect of compound **2** on Hsp27. SKBR-3 breast cancer cells were treated with DMSO, **2**, nocodozole, and an Hsp27 inhibitor with various concentrations for 24 h. Total cell lysates were extracted using M-PER reagent (Pierce). Equal amounts of proteins (50 μg) were separated by SDS−PAGE and transferred onto PVDF membrane. The membranes were blocked for 1 h, followed by being probed with the respective primary antibodies (anti-Hsp27, anti-pSer78 Hsp27, and antiactin) and secondary antibody.

pHsp27 levels, which was similar to the response after tubulin inhibitor nocodazole treatment. Cells use pHsp27 as a protective molecule when any damage happens to the cells.[35,42] It is very common that cells express a higher level of pHsp27 after being treated with cytotoxic agents.[43] Compound **2** inhibited tubulin polymerization and induced cell death, which is very likely to promote the activation of pHsp27 in the cells. KRIBB3,[44] an Hsp27 binder, also retained Hsp27 protein via its biotinylated probe in a protein pull-down assay. It was used as a control, and it significantly inhibited Hsp27 phosphorylation (Figure 7). It seemed that compound **2** showed a different manner to this known Hsp27 binder regarding Hsp27 inhibition, suggesting that compound **2** might bind to a different domain of Hsp27 and that this domain was not involved in Hsp27 phosphorylation. It was also possible that the tubulin inhibitory activity of compound **2** dramatically induced Hsp27 phosphorylation and overrode the direct Hsp27 inhibitory effect of the compound. Tubulin function was relatively easier to check with a polymerization assay. However, it was difficult to elucidate whether Hsp27 was an anticancer target for compound **2**. Besides Hsp27 phosphorylation, the other downstream molecular and cellular consequences of Hsp27 inhibition were not well-defined. The tubulin inhibition could lead to Hsp27 phosphorylation, as indicated by pure tubulin inhibitor nocodazole in Figure 7, suggesting that tubulin function had a close correlation to Hsp27 function. It also made it difficult to solely investigate the Hsp27 effects of the dual targets compound **2**. More medicinal chemistry effort is needed to develop more specific ligands and dissociate the two targets of compound **2**.

2.5. Docking with Tubulin. Compound **2** bound to tubulin and inhibited polymerization, which led to abnormal cell function and ultimately cell death. Our studies also suggest that compound **2** is a colchicine domain binder on tubulin. To further elucidate the binding characters of the compound with tubulin, we performed docking studies with compound **2** at the colchicine binding pocket (Figure 8A). It has been reported that colchicine mainly interacts with β-tubulin.[42,45] Our docking investigation suggests that compound **2** interacted with both α- and β-tubulin in the colchicine pocket. The sulfonamide group of the compound formed a dipole−dipole interaction with Tyr224 (α-tubulin). The 2, 5-dimethylbenzyl moiety made hydrophobic contacts with the Tyr224 and Ser178 residues located on the α-tubulin (Figure 8B). The piperonylic amide moiety formed a hydrophobic interaction with Leu248 (β-tubulin). The three interactions contributed to the strong binding affinity of the compound to tubulin and subsequently led to the tubulin polymerization inhibition activity. Negative compound **4** without the 2,5-dimethyl groups on the benzyl ring lost the three interactions (Figure 8C). A new hydrophobic interaction (Asn 258 interacted with the central benzene ring) was formed because of the molecule shifting from the pocket (Figure 8D), but the interaction was weak compared to the three interactions of compound **2**. Compound **4** inhibited SKBR-3 breast cancer cell growth with an IC_{50} of 62.9 μM. In addition, negative compound **5** with a benzylamide moiety instead of piperonylic amide moiety only interacted with Ser178, even though the dimethyl group was maintained in the structure (Figure 8E). The longer side chain of the amide moiety pushed the 2,5-dimethylbenzyl moiety away from the pocket and forced the molecule to rotate in the binding domain. Compared with **2**, the benzyl and the sulfonamide moieties of compound **5** switched (Figure 8F), and therefore, the molecule lost its interaction with TyrA224 and Leu248. The only interaction between the compound and the binding pocket was the central benzene ring with Ser178, which led to a weaker tubulin inhibitor. Compound **5** inhibited SKBR-3 breast cancer cell growth with an IC_{50} of 120.8 μM. These results further demonstrated that compound **2** bound at the colchicine binding site of tubulin and that the dimethylbenzyl and the benzamide moieties of the compound were very important for anticancer activity.

3. CONCLUSION

A class of new anticancer agents were developed based on the COX-2 inhibitor nimesulide as a lead compound.[20] To identify the molecular targets of the agents and elucidate the anticancer mechanism, we designed and synthesized the biotinylated nimesulide analogue **2** as a probe. The proteins binding with the compound were isolated and subjected to mass spectrometric identification, and the most prevalent binding proteins were determined to be tubulin and Hsp27. Both proteins are very important for cancer cell proliferation. Further investigation revealed that the compound bound at colchicine binding domain on tubulin and interrupted the polymerization of tubulin. However, the biological activity of compound **2** on Hsp27 was difficult to determine because the tubulin inhibitory activity of compound **2** stimulated the activation of Hsp27 signals. The direct Hsp27 inhibitory effects of compound **2** could be overridden by the tubulin inhibition consequences. Studies are now underway to further optimize compound **2** in order to generate more potent derivatives. In addition, more specific ligands, which have dissociated targets, i.e., pure tubulin inhibitor or pure Hsp27 inhibitor, might be identified from the pool of new compounds. The new sole ligands will allow us to further investigate the consequences of Hsp27 inhibition.

4. EXPERIMENTAL SECTION

4.1. Biotinylation of Compound 2. Chemicals were commercially available and used as received without further purification unless otherwise noted. Moisture sensitive reactions were carried out under a dry argon atmosphere in flame-dried glassware. Solvents were distilled before use under argon. Thin-layer chromatography was performed on precoated silica gel F254 plates (Whatman). Silica gel column

dx.doi.org/10.1021/jm300100d | J. Med. Chem. 2012, 55, 3425−3435

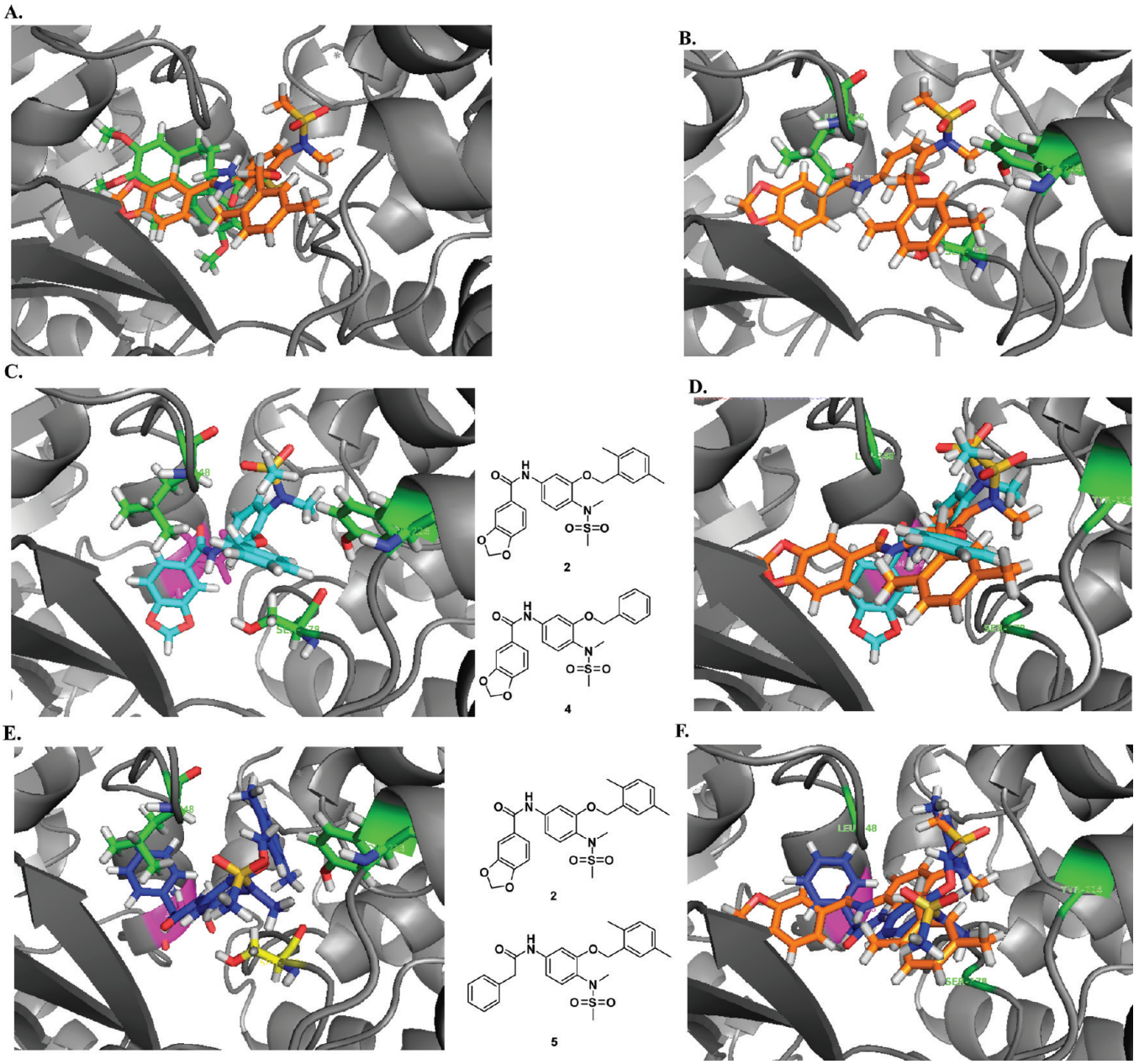

Figure 8. (A) Compound **2** (orange) and colchicine (Green) share the same binding site on tubulin. The left part of the imagine is β-tubulin, and the right part is α-tubulin. (B) There are several interactions between **2** and the binding pocket including the 2,5-dimethylbenzyl moiety interacting with Ser178 and Tyr224 (α-tubulin), the sulfonamide group interacting with Tyr224, and the piperonylic amide group interacting with Leu 248 located on β-tubulin (all three green residues). (C) Negative compound **4** (inhibiting SKBR-3 cell growth with an IC_{50} of 62.9 μM) does not have the 2,5-dimethyl group on the benzyl moiety. The compound does not interact with the three sites identified with **2**. It only interacts with Asn 258 (magenta), which makes it loosely sits in the pocket. (D) Comparison of **2** and negative **4**. Without the dimethyl groups on the benzyl ring, the moiety does not interact with Ser178, and the whole molecule (cyan) slightly shifts away from the **2** (orange) binding site. From the SAR generated in the previous studies on this series of compounds, the dimethyl group is very critical for anticancer activity. It matches this docking result. (E) Negative compound **5** (inhibiting SKBR-3 cell growth with an IC_{50} of 120.8 μM) has a benzylamide moiety instead of piperonylic amide moiety. Interestingly, the compound docks in the pocket in a different mode. Compared with **2**, the benzyl and the sulfonamide moieties switch binding domain. However, the compound only has an interaction with Ser178 (yellow), which leads to a weak tubulin inhibitor. (F) Comparison of **2** and negative **5**. Changing piperonylic amide moiety to benzylamide leads to a rotation of the molecule (blue) in the docking site compared to **2** (orange). The Ser178 residue interacts with the central benzene ring of the negative compound, and this is the only interaction of the molecule with the docking site.

chromatography was performed using silica gel 60A (Merck, 230–400 mesh), and hexane/ethyl acetate was used as the elusion solvent. Mass spectra were obtained on the Micromass quadrupole time-of-flight (QTOF) electrospray mass spectrometer at Cleveland State University MS Facility Center. All the NMR spectra were recorded on a Varian 400 MHz in either DMSO-d_6 or $CDCl_3$. Chemical shifts (δ) for ^{1}H NMR spectra are reported in parts per million to residual solvent protons.

Negative compounds **4** and **5**, compounds **I** and **II**, and the methodology of the probe synthesis were described in previous studies (Scheme 1).[20,46]

*Benzo[1,3]dioxole-5-carboxylic Acid [3-(2,5-Dimethylbenzyloxy)-4-(methanesulfonylamino)phenyl]amide (**III**).* A mixture of ferric chloride (4 mmol, 4 equiv) and **II** (1 mmol, 1 equiv) was added to a solvent mixture of DMF/water (3:1, 8 mL). It was stirred for 15 min,

dx.doi.org/10.1021/jm300100d | J. Med. Chem. 2012, 55, 3425–3435

and then zinc dust (10 mmol, 10 equiv) was added slowly. The mixture was stirred at room temperature for half an hour and then filtered by passing it through a Celite pad. The filtrate was diluted with water. The precipitated solid was collected by filtration, and then it was dissolved in acetone. After filtration of the insoluble residue, the filtrate was collected and concentrated under vacuum to afford the substituted aniline. To the substituted aniline (1.0 mmol, 1.0 equiv) in 3 mL of 1,4-dioxane were added K_2CO_3 (5 mmol, 5 equiv) and piperonyloyl chloride (1.2 mmol, 1.2 equiv), and the mixture was stirred at room temperature overnight. Then 10 mL of H_2O and 3 mL of saturated aqueous Na_2CO_3 were added to the mixture, and the mixture was stirred at room temperature overnight. The precipitated solid was collected by filtration and recrystallized in ethanol. ^{1}H NMR (400 MHz, DMSO-d_6) δ 10.120 (1H, s), 8.915 (1H, s), 7.720 (1H, d, J = 2.4 Hz), 7.575 (1H, dd, J = 1.6, 8 Hz), 7.513 (1H, d, J = 1.6 Hz), 7.379 (2H, m), 7.207 (1H, d, J = 8.8 Hz), 7.080 (3H, m), 6.140 (2H, s), 5.064 (2H, s), 2.847 (3H, s), 2.318 (3H, s), 2.283 (3H, s).

*Benzo[1,3]dioxole-5-carboxylic Acid {3-(2,5-Dimethylbenzyloxy)-4-[(6-hydroxyhexyl)methanesulfonylamino]phenyl}amide (**IV**).* K_2CO_3 (5 mmol, 5 equiv) and 6-bromo-1-hexanol (1.2 mmol, 1.2 equiv) were successively added to a solution of **III** (1.0 mmol, 1.0 equiv) in 3 mL of DMF, and the mixture was stirred at room temperature overnight. An amount of 12 mL of H_2O was added, and the precipitated solid was collected by filtration and purified by flash column chromatography. ^{1}H NMR (400 MHz, $CDCl_3$) δ 8.227 (1H, s), 7.962 (1H, d, J = 2 Hz), 7.455 (1H, dd, J = 1.6, 8 Hz), 7.388 (1H, d, J = 1.6 Hz), 7.220 (1H, d, J = 8.4 Hz), 7.091 (3H, m), 6.853 (2H, m), 6.047 (2H, s), 5.035 (2H, s), 3.575 (2H, t, J = 6.4 Hz), 3.515 (2H, br), 2.714 (3H, s), 2.315 (6H, s), 1.504−1.287 (8H, m).

*N-(3-(2,5-Dimethylbenzyloxy)-4-(N-(6-(5-((3aR,4R,6aS)-2-oxohexahydro-1H-thieno[3,4-d]imidazol-4-yl)pentanamido)hexyl)methylsulfonamido)phenyl)benzo[d][1,3]dioxole-5-carboxamide (**V**).* To a solution of **IV** (2 mmol, 1 equiv) and triethylamine (10 mmol, 5 equiv) in dichloromethane (5 mL) at 0 °C was added methylsulfonyl chloride (6 mmol, 3 equiv). The mixture was kept stirring at room temperature. After the reaction was completed, ice cold water was added to the solution. The organic layer was washed twice with ice cold water and then evaporated to give mesylated **IV**. A solution of this intermediate in ethanol (20 mL) and ammonium hydroxide (20 mL) was stirred for 2 days at room temperature and then concentrated to give the intermediate amine, which was used for the next step directly without purification. To the mixture of amine (2 mmol, 1 equiv) and biotin (2 mmol, 1 equiv) and PyBOP (2 mmol, 1 equiv) in 5 mL of DMF was added triethylamine (4 mmol, 2 equiv), and the mixture was stirred at room temperature for 2 h. An amount of 15 mL of H_2O was added to the mixture, and the precipitated solid was filtered and purified by flash column chromatography. ^{1}H NMR (400 MHz, $CDCl_3$) δ 8.864 (1H, s), 8.058 (1H, s), 7.526 (1H, d, J = 8 Hz), 7.457 (1H, s), 7.235 (1H, d, J = 8.4 Hz), 7.090 (3H, m), 6.976 (1H, dd, J = 2, 8.4 Hz), 6.871 (1H, d, J = 8 Hz), 6.277 (1H, s), 6.229 (1H, t, J = 5.6 Hz), 6.040 (2H, s), 5.345 (1H, s), 5.060 (2H, s), 4.455 (1H, m), 4.260 (1H, m), 3.500 (2H, br), 3.113 (3H, m), 2.866 (1H, dd, J = 4.8, 12.8 Hz), 2.704 (4H, m), 2.322 (3H, s), 2.315 (3H, s), 2.165 (2H, t, J = 7.6 Hz), 1.692−1.253 (14H, m). ESI-MS calcd for $C_{40}H_{52}N_5O_8S_2$ $[M + H]^+$ 794.3, found 794.2

4.2. Biological Studies. *4.2.1. Cell Culture.* SKBR-3 cells were obtained from ATCC (Rockville, MD). The cells were maintained in RPMI 1640 medium supplemented with 10% fetal bovine serum (FBS), 2 mmol/L L-glutamine, 1 mmol/L sodium pyruvate, and 100 U/mL penicillin−streptomycin. FBS was heat inactivated for 30 min in a 56 °C water bath before use. Cell cultures were grown at 37 °C in a humidified atmosphere of 5% CO_2 in a Hereaus CO_2 incubator.

4.2.2. Cell Viability Analysis. The effects of compounds **4**, **5**, **2**, and its biotinylated probe on SKBR-3 cell viability were assessed using the 3-(4,5-dimethylthiazol-2-yl)-2,5-diphenyl-2*H*-tetrazolium bromide assay in six replicates. Cells were grown in RPMI 1640 medium in 96-well, flat-bottomed plates for 24 h and were exposed to various concentrations of the compounds dissolved in DMSO (final concentration of ≤0.1%) in medium for 48 h. Controls received DMSO vehicle at a concentration equal to that in drug-treated cells. The medium was removed, replaced by 200 μL of 0.5 mg/mL 3-(4,5-dimethylthiazol-2-yl)-2,5-diphenyl-2*H*-tetrazolium bromide in fresh medium, and cells were incubated in the CO_2 incubator at 37 °C for 2 h. Supernatants were removed from the wells, and the reduced 3-(4,5-dimethylthiazol-2-yl)-2,5-diphenyl-2*H*-tetrazolium bromide dye was solubilized in 200 μL/well DMSO. Absorbance at 570 nm was determined on a plate reader. Statistical and graphical information was determined using GraphPad Prism software (GraphPad Software Incorporated) and Microsoft Excel (Microsoft Corporation). Determination of IC_{50} values was performed using nonlinear regression analysis.

4.2.3. Biotin−Neutravidin Pull-Down Assay. SKBR-3 cells (1.0×10^7) were disrupted in a NP-40 lysis buffer and sonicated with freshly added protease inhibitor cocktail (Roche). The cell lysate was incubated with biotin-conjugated compound **2** probe at room temperature for 1 h. The mixture was further incubated with equilibrated and packed neutravidin resin in columns at room temperature for 30 min, which was followed by centrifugation and five times repeated washing with binding buffer to wash out nonbinding proteins. The pull-down assay was performed according to the protocol of neutravidin (Thermofisher). The protein interacting with the biotinylated compound **2** was cleaved from the beads by eluting with binding buffer containing compound **2**. The resin was also collected and boiled with SDS buffer to determine the leftover proteins. The elution solution was boiled with 1× loading buffer (100 mmol/L DTT plus bromophenol blue) for 5 min and then electrophoresed on a 10% SDS−polyacrylamide gel. The resulting gel was visualized with silver stain kit (for mass spectrometry, compatible silver staining kit, Invitrogen).

*4.2.4. Peptide Analysis of the **2**-Binding Protein via Mass Spectrometry.* Bands visualized by silver staining were cut and transferred to 0.65 mL siliconized tubes (National Scientific Supply, Claremont, CA, U.S.). The silver reagent was removed with the denatured reagents (Invitrogen). Proteins were in-gel digested by trypsin (sequencing grade, modified; Promega, Madison, WI, U.S.). The protein digest was reconstituted in 20 μL of 0.1% (v/v) trifluoroacetic acid prior to LC-QTOF/MS analysis. Peptide separation was carried out using a 10 μL sample injection at 50 μL/min flow rate on a Vydac protein and peptide C18 (5 μm, 300 Å, 1 mm × 150 mm) column (Grace Discovery Sciences, Deerfield, IL, U.S.) preceded by an inline filter (0.5 μm pore) (Upchurch Scientific, Oak Harbor, WA, U.S.). The gradient elution profile consisted of 1% of mobile phase A for 5 min, then brought to 60% of mobile phase B over 90 min, and followed by 90% of mobile phase B for 8 min. The total run time was 105 min. Mobile phase A was 0.1% (v/v) formic acid in HPLC-grade doubly distilled H_2O, and mobile phase B was 0.1% (v/v) formic acid in HPLC-grade acetonitrile. Peptide detection was done using the positive information-dependent-acquisition (IDA) mode of AB Sciex QStar Elite Q-TOF mass spectrometer (AB Sciex, Foster City, CA, U.S.). Data acquisition was performed using AB Sciex Analyst QS (version 2.0). Protein identification through peptides matching was accomplished using Mascot MS/MS ions search (http://www.matrixscience.com).

4.2.5. Western Blot. To confirm the identity of protein targets that have been discovered in neutravidin resin pull-down assay, Western blot was conducted. Protein samples were separated on 12% SDS−polyacrylmide gel and transferred onto polyvinylidene difluoride (PVDF) membrane (Pall Cooperation, FL). After blocking, the membrane was incubated in PBST containing 5% BSA and primary antibody specific to α-, β-tubulin or Hsp27 (Cell Signaling, MA) overnight at 4 °C. HRP-conjugated anti-rabbit IgG or anti-mouse IgG (Cell Signaling, MA) was used as secondary antibody and incubated at room temperature for 1 h. Membrane was incubated in ECL plus reagent (GE health) and then exposed to hyper film.

To determine the effect of compound **2** on Hsp27 phosphorylation, SKBR-3 cells were treated with 0.2, 0.5, and 1 μM compound **2**, 50 and 100 nM nocodazole (Sigma), and 0.5 and 1 μM KRIBB3 (Sigma) for 24 h. Extracted proteins from SKBR-3 cells were loaded on 12% SDS−polyacrylamide gel. Antibody specific to phosphorylated

Hsp27 (Ser 78, Cell Signaling, MA) was used to blot membrane, and secondary antibody anti-rabbit IgG was blotted thereafter. Hsp27 and actin antibodies were also used to confirm equal loading amount.

4.2.6. 2 Binding to Tubulin and Hsp27. 10 μM bovine brain tubulin (Cytoskeleton, Denver, CO) or recombinant Hsp27 (ProSpec, East Brunswick, NJ) was incubated with 2 μM biotinylated compound **2** in binding buffer in a total volume of 500 μL for 1 h at room temperature before loading onto prepacked neutravidin resin column and further incubated for 30 min. The resin was washed with 500 μL of binding buffer 5 times and 2 times with buffer containing compound **2**. For the colchicine, paclitaxel, and compound **2** probe competition experiments, tubulin was preincubated with 10 μM colchicine or paclitaxel at room temperature for 1 h before the incubation with the probe. The samples were fractionated by SDS−PAGE and examined with Western blot assay.

4.2.7. Tubulin Polymerization Assay. Microtubule-associated protein-rich tubulin (2 mg/mL, bovine brain, Cytoskeleton) in buffer containing 80 mM PIPES (pH 6.9), 2 mM $MgCl_2$, 0.5 mM EGTA, and 5% glycerol was placed in cuvettes, 200 μL/assay, and incubated respectively with DMSO, 0.5 and 1 μM compound **2**, 5 μM compound **3**, and 3 μM nacodazole. Polymerization was started by adding 1 mM GTP and incubating at 37 °C, followed by absorption readings at 340 nm with a Varian Cary 50 series spectrophotometer (every 5 s/min 0 to min 3, every 10 s/min 3 to min 5, every 30 s/min 5 to min 10, and every 60 s/min 10 to min 17).

4.2.8. Indirect Immunofluorescence Staining. SKBR-3 cells were transferred in chamber slides and cultured to 70% confluence and then incubated with 0.5 or 1 μM compound **2** respectively for 12 and 24 h. In parallel, the cells without treatment were used as negative control, and cells treated with 0.05 μM nacodazole for 12 and 24 h were used as positive control. Cells receiving different treatments were fixed in 4% paraformaldehyde for 10 min at room temperature and then permeabilized with 0.2% Triton X-100 for another 10 min. After blocking with 2% goat serum for 45 min at room temperature, cells were incubated with biotinylated anti-tubulin antibody (1:200, Molecular Probes) overnight at 4 °C. After being washed with PBS, cells were then stained with Alexa Fluor 488 streptavidin (1:1000, Invitrogen) for 45 min at room temperature, which was followed by mounting with antifade reagent (ProLong Gold antifade reagent, Invitrogen). Fluorescently stained cells were analyzed with a Leica TCS SP2 fluorescence microscope.

4.2.9. Docking Investigation. Docking studies were done to gain insight into the possible mode of interaction between the compounds and tubulin. The structures were drawn with Marvin Sketch (www.ChemAxon.com) and energy minimized in MOE 2010 (www.chemcomp.com) using the MMFF94s force field. The database of compounds was then used for the docking studies. The protein crystal structure of 1SAO.pdb was prepared for docking by adjusting the pH of the system to pH 7.4.[45] The binding site in tubulin was delineated by colchicine. After docking, only the top docked pose of each compound was retained for analysis.

AUTHOR INFORMATION

Corresponding Author

*Phone: 216-687-9219. Fax: 216-687-9298. Email: B.su@csuohio.edu.

Notes

The authors declare no competing financial interest.

ACKNOWLEDGMENTS

This research was supported by a startup fund from Cleveland State University, OH. We thank Dr. Xue-long Sun (Cleveland State University) for help on the UV analysis of tubulin polymerization, and Jones Sidney (Department of Molecular Cardiology, Cleveland Clinic, OH) on the cellular microtubule images taken.

ABBREVIATIONS USED

COX-2, cyclooxygenase-2; Hsp27, heat shock protein 27; sHsp, small heat shock protein; FDA, Food and Drug Administration; SDS−PAGE, sodium dodecyl sulfate−polyacrylamide gel electrophoresis; QTOF, quadrupole time-of-flight; FBS, fetal bovine serum; PVDF, polyvinylidene difluoride

REFERENCES

(1) Heald, R.; Nogales, E. Microtubule dynamics. *J. Cell Sci.* **2002**, *115*, 3−4.
(2) Rowinsky, E. K. Paclitaxel pharmacology and other tumor types. *Semin. Oncol.* **1997**, *24*, S19-1−S19-12.
(3) Kuppens, I. E. Current state of the art of new tubulin inhibitors in the clinic. *Curr. Clin. Pharmacol.* **2006**, *1*, 57−70.
(4) Orr, G. A.; Verdier-Pinard, P.; McDaid, H.; Horwitz, S. B. Mechanisms of Taxol resistance related to microtubules. *Oncogene* **2003**, *22*, 7280−7295.
(5) Perez, E. A. Microtubule inhibitors: differentiating tubulin-inhibiting agents based on mechanisms of action, clinical activity, and resistance. *Mol. Cancer Ther.* **2009**, *8*, 2086−2095.
(6) Perez, E. A. Impact, mechanisms, and novel chemotherapy strategies for overcoming resistance to anthracyclines and taxanes in metastatic breast cancer. *Breast Cancer Res. Treat.* **2009**, *114*, 195−201.
(7) Carlson, K.; Ocean, A. J. Peripheral neuropathy with microtubule-targeting agents: occurrence and management approach. *Clin. Breast Cancer.* **2011**, *11*, 73−81.
(8) Swain, S. M.; Arezzo, J. C. Neuropathy associated with microtubule inhibitors: diagnosis, incidence, and management. *Clin. Adv. Hematol. Oncol.* **2008**, *6*, 455−467.
(9) Wozniak, K. M.; Nomoto, K.; Lapidus, R. G.; Wu, Y.; Carozzi, V.; Cavaletti, G.; Hayakawa, K.; Hosokawa, S.; Towle, M. J.; Littlefield, B. A.; Slusher, B. S. Comparison of neuropathy-inducing effects of eribulin mesylate, paclitaxel, and ixabepilone in mice. *Cancer Res.* **2011**, *71*, 3952−3962.
(10) Britten, C. D.; Baker, S. D.; Denis, L. J.; Johnson, T.; Drengler, R.; Siu, L. L.; Duchin, K.; Kuhn, J.; Rowinsky, E. K. Oral paclitaxel and concurrent cyclosporin A: targeting clinically relevant systemic exposure to paclitaxel. *Clin. Cancer Res.* **2000**, *6*, 3459−3468.
(11) Lee, J. J.; Kelly, W. K. Epothilones: tubulin polymerization as a novel target for prostate cancer therapy. *Nat. Clin. Pract. Oncol.* **2009**, *6*, 85−92.
(12) Bollag, D. M.; McQueney, P. A.; Zhu, J.; Hensens, O.; Koupal, L.; Liesch, J.; Goetz, M.; Lazarides, E.; Woods, C. M. Epothilones, a new class of microtubule-stabilizing agents with a Taxol-like mechanism of action. *Cancer Res.* **1995**, *55*, 2325−2333.
(13) Bai, R.; Nguyen, T. L.; Burnett, J. C.; Atasoylu, O.; Munro, M. H.; Pettit, G. R.; Smith, A. B. 3rd; Gussio, R.; Hamel, E. Interactions of halichondrin B and eribulin with tubulin. *J. Chem. Inf. Model.* **2011**, *51*, 1393−1404.
(14) Bai, R. L.; Paull, K. D.; Herald, C. L.; Malspeis, L.; Pettit, G. R.; Hamel, E. Halichondrin B and homohalichondrin B, marine natural products binding in the vinca domain of tubulin. Discovery of tubulin-based mechanism of action by analysis of differential cytotoxicity data. *J. Biol. Chem.* **1991**, *266*, 15882−15889.
(15) Horwitz, S. B.; Cohen, D.; Rao, S.; Ringel, I.; Shen, H. J.; Yang, C. P. Taxol: mechanisms of action and resistance. *J. Natl. Cancer. Inst. Monogr.* **1993**, *15*, 55−61.
(16) Bacher, G.; Nickel, B.; Emig, P.; Vanhoefer, U.; Seeber, S.; Shandra, A.; Klenner, T.; Beckers, T. D-24851, a novel synthetic microtubule inhibitor, exerts curative antitumoral activity in vivo, shows efficacy toward multidrug-resistant tumor cells, and lacks neurotoxicity. *Cancer Res.* **2001**, *61*, 392−399.
(17) Beckers, T.; Reissmann, T.; Schmidt, M.; Burger, A. M.; Fiebig, H. H.; Vanhoefer, U.; Pongratz, H.; Hufsky, H.; Hockemeyer, J.; Frieser, M.; Mahboobi, S. 2-Aroylindoles, a novel class of potent, orally active small molecule tubulin inhibitors. *Cancer Res.* **2002**, *62*, 3113−3119.

(18) Hande, K. R.; Hagey, A.; Berlin, J.; Cai, Y.; Meek, K.; Kobayashi, H.; Lockhart, A. C.; Medina, D.; Sosman, J.; Gordon, G. B.; Rothenberg, M. L. The pharmacokinetics and safety of ABT-751, a novel, orally bioavailable sulfonamide antimitotic agent: results of a phase 1 study. *Clin. Cancer Res.* **2006**, *12*, 2834−2840.
(19) Su, B.; Darby, M. V.; Brueggemeier, R. W. Synthesis and biological evaluation of novel sulfonanilide compounds as antiproliferative agents for breast cancer. *J. Comb. Chem.* **2008**, *10*, 475−483.
(20) Zhong, B.; Cai, X.; Chennamaneni, S.; Yi, X.; Liu, L.; Pink, J. J.; Dowlati, A.; Xu, Y.; Zhou, A.; Su, B. From COX-2 inhibitor nimesulide to potent anti-cancer agent: synthesis, in vitro, in vivo and pharmacokinetic evaluation. *Eur. J. Med. Chem.* **2012**, *47*, 432−444.
(21) Baoping, Y.; Guoyong, H.; Jieping, Y.; Zongxue, R.; Hesheng, L. Cyclooxygenase-2 inhibitor nimesulide suppresses telomerase activity by blocking Akt/PKB activation in gastric cancer cell line. *Dig. Dis. Sci.* **2004**, *49*, 948−953.
(22) Elder, D. J.; Halton, D. E.; Hague, A.; Paraskeva, C. Induction of apoptotic cell death in human colorectal carcinoma cell lines by a cyclooxygenase-2 (COX-2)-selective nonsteroidal anti-inflammatory drug: independence from COX-2 protein expression. *Clin. Cancer Res.* **1997**, *3*, 1679−1683.
(23) Hanif, R.; Pittas, A.; Feng, Y.; Koutsos, M. I.; Qiao, L.; Staiano-Coico, L.; Shiff, S. I.; Rigas, B. Effects of nonsteroidal anti-inflammatory drugs on proliferation and on induction of apoptosis in colon cancer cells by a prostaglandin-independent pathway. *Biochem. Pharmacol.* **1996**, *52*, 237−245.
(24) Johnson, A. J.; song, X.; Hsu, A.; Chen, C. Apoptosis signaling pathways mediated by cyclooxygenase-2 inhibitors in prostate cancer cells. *Adv. Enzyme Regul.* **2001**, *41*, 221−235.
(25) Pan, Y.; Zhang, J. S.; Gazi, M. H.; Young, C. Y. The cyclooxygenase 2-specific nonsteroidal anti-inflammatory drugs celecoxib and nimesulide inhibit androgen receptor activity via induction of c-Jun in prostate cancer cells. *Cancer Epidemiol., Biomarkers Prev.* **2003**, *12*, 769−774.
(26) Shiff, S. J.; Koutsos, M. I.; Qiao, L.; Rigas, B. Nonsteroidal antiinflammatory drugs inhibit the proliferation of colon adenocarcinoma cells: effects on cell cycle and apoptosis. *Exp. Cell Res.* **1996**, *222*, 179−188.
(27) Alberts, D. S.; Hixson, L.; Ahnen, D.; Bogert, C.; Einspahr, J.; Paranka, N.; Brendel, K.; Gross, P. H.; Pamukcu, R.; Burt, R. W. Do NSAIDs exert their colon cancer chemoprevention activities through the inhibition of mucosal prostaglandin synthetase? *J. Cell. Biochem. Suppl.* **1995**, *22*, 18−23.
(28) Julemont, F.; de Leval, X.; Michaux, C.; Damas, J.; Charlier, C.; Durant, F.; Pirotte, B.; Dogne, J. M. Spectral and crystallographic study of pyridinic analogues of nimesulide: determination of the active form of methanesulfonamides as COX-2 selective inhibitors. *J. Med. Chem.* **2002**, *45*, 5182−5185.
(29) Su, B.; Diaz-Cruz, E. S.; Landini, S.; Brueggemeier, R. W. Novel sulfonanilide analogues suppress aromatase expression and activity in breast cancer cells independent of COX-2 inhibition. *J. Med. Chem.* **2006**, *49*, 1413−1419.
(30) Boelsterli, U. A.; Ho, H. K.; Zhou, S.; Leow, K. Y. Bioactivation and hepatotoxicity of nitroaromatic drugs. *Curr. Drug Metab.* **2006**, *7*, 715−727.
(31) Zhong, B.; Cai, X.; Yi, X.; Zhou, A.; Chen, S.; Su, B. In vitro and in vivo effects of a cyclooxygenase-2 inhibitor nimesulide analog JCC76 in aromatase inhibitors-insensitive breast cancer cells. *J. Steroid Biochem. Mol. Biol.* **2011**, *126*, 10−18.
(32) Chen, B.; Su, B.; Chen, S. A COX-2 inhibitor nimesulide analog selectively induces apoptosis in Her2 overexpressing breast cancer cells via cytochrome *c* dependent mechanisms. *Biochem. Pharmacol.* **2009**, *77*, 1787−1794.
(33) Rix, U.; Superti-Furga, G. Target profiling of small molecules by chemical proteomics. *Nat. Chem. Biol.* **2009**, *5*, 616−624.
(34) Zhong, B.; Lama, R.; Smith, K. M.; Xu, Y.; Su, B. Design and synthesis of a biotinylated probe of COX-2 inhibitor nimesulide analog JCC76. *Bioorg. Med. Chem. Lett.* **2011**, *21*, 5324−5327.
(35) Sherman, M.; Multhoff, G. Heat shock proteins in cancer. *Ann. N.Y. Acad. Sci.* **2007**, *1113*, 192−201.
(36) Hino, M.; Kurogi, K.; Okubo, M. A.; Murata-Hori, M.; Hosoya, H. Small heat shock protein 27 (HSP27) associates with tubulin/microtubules in HeLa cells. *Biochem. Biophys. Res. Commun.* **2000**, *271*, 164−169.
(37) Rowinsky, E. K. Current developments in antitumor antibiotics, epipodophyllotoxins, and vinca alkaloids. *Curr. Opin. Oncol.* **1991**, *3*, 1060−1069.
(38) Nettles, J. H.; Li, H.; Cornett, B.; Krahn, J. M.; Snyder, J. P.; Downing, K. H. The binding mode of epothilone A on alpha,beta-tubulin by electron crystallography. *Science* **2004**, *305*, 866−869.
(39) Bruey, J. M.; Ducasse, C.; Bonniaud, P.; Ravagnan, L.; Susin, S. A.; Diaz-Latoud, C.; Gurbuxani, S.; Arrigo, A. P.; Kroemer, G.; Solary, E.; Garrido, C. Hsp27 negatively regulates cell death by interacting with cytochrome *c*. *Nat. Cell Biol.* **2000**, *2*, 645−652.
(40) Bruey, J. M.; Paul, C.; Fromentin, A.; Hilpert, S.; Arrigo, A. P.; Solary, E.; Garrido, C. Differential regulation of HSP27 oligomerization in tumor cells grown in vitro and in vivo. *Oncogene* **2000**, *19*, 4855−4863.
(41) Langer, R.; Ott, K.; Specht, K.; Becker, K.; Lordick, F.; Burian, M.; Herrmann, K.; Schrattenholz, A.; Cahill, M. A.; Schwaiger, M.; Hofler, H.; Wester, H. J. Protein expression profiling in esophageal adenocarcinoma patients indicates association of heat-shock protein 27 expression and chemotherapy response. *Clin. Cancer Res.* **2008**, *14*, 8279−8287.
(42) Sun, Y.; MacRae, T. H. The small heat shock proteins and their role in human disease. *FEBS J.* **2005**, *272*, 2613−2627.
(43) Casado, P.; Zuazua-Villar, P.; Prado, M. A.; Valle, E. D.; Iglesias, J. M.; Martinez-Campa, C.; Lazo, P. S.; Ramos, S. Characterization of HSP27 phosphorylation induced by microtubule interfering agents: implication of p38 signalling pathway. *Arch. Biochem. Biophys.* **2007**, *461*, 123−129.
(44) Shin, K. D.; Lee, M. Y.; Shin, D. S.; Lee, S.; Son, K. H.; Koh, S.; Paik, Y. K.; Kwon, B. M.; Han, D. C. Blocking tumor cell migration and invasion with biphenyl isoxazole derivative KRIBB3, a synthetic molecule that inhibits Hsp27 phosphorylation. *J. Biol. Chem.* **2005**, *280*, 41439−41448.
(45) Ravelli, R. B.; Gigant, B.; Curmi, P. A.; Jourdain, I.; Lachkar, S.; Sobel, A.; Knossow, M. Insight into tubulin regulation from a complex with colchicine and a stathmin-like domain. *Nature* **2004**, *428*, 198−202.
(46) Su, B.; Tian, R.; Darby, M. V.; Brueggemeier, R. W. Novel sulfonanilide analogs decrease aromatase activity in breast cancer cells: synthesis, biological evaluation, and ligand-based pharmacophore identification. *J. Med. Chem.* **2008**, *51*, 1126−1135.